Mathematical Theory and Modeling
ISSN 2224-5804 (Paper) ISSN 2225-0522 (Online)
Vol.11, No.5, 2021

Effect of Climatic Governing Parameters on the Performance of Solar Adsorption Refrigeration System

[1] Emmanuel O. Sangotayo, [2]Mufutau A. Waheed, [3]Solomon O. Alagbe, [4*]Olukunle E. Itabiyi
1,4. Department of Mechanical Engineering, Ladoke Akintola University of Technology,
P. M. B. 4000, Ogbomoso, Nigeria.
2. Department of Mechanical Engineering, College of Engineering, Federal University of Agriculture,
P. M. B. 2240, Abeokuta, Nigeria.
3. Department of Chemical Engineering, Ladoke Akintola University of Technology,
P. M. B. 4000, Ogbomoso, Nigeria.
Corresponding author[*] - oeitabiyi@lautech.edu.ng

Abstract

Solar energy is a renewable resource, clean and ecologically friendly. Solar thermal energy is attractive alternative energy to drive the adsorption of refrigeration machines. This work presents a numerical investigation of the effect of climatic governing parameters such as ambient temperature and component temperatures on the performance of solar adsorption refrigeration systems using methanol/activated charcoal pairs.

Activated carbon as adsorbent and methanol as a refrigerant is selected. Some predictive empirical equations accounting for heat balance in the solar collector components, instantaneous heat and mass transfer in adsorbent bed, and performance parameters were presented. Interactive C++ programming was developed to carry out the parametric study of some climatic factors such as ambient temperature and solar radiation intensity with aperture width of 0.14 m, collector length of 2.1m on the system performance. The effect of ambient temperature and component temperatures with aperture width, collector length, on specific cooling power (SCP), refrigeration cycle COP (COP_{cycle}), and solar coefficient of performance (COPs) are being investigated. The results are presented in form of profiles such as pressure developed in the generator, specific cooling power and system coefficient of performance profiles, under varying weather conditions and ambient temperature, operating conditions of evaporating temperature, T_{ev} = 0 ^oC, condensing temperature, T_{con} = 30 ^oC and desorption temperature of 100 ^oC,

The influences of operating and design parameters on the system performance are significant. The system performance shows no appreciable changes with varying condenser temperature with significant effect with varying evaporation and desorption temperature. It is shown clearly that for different desorption temperatures below 120 ^oC there is an appreciable effect on the system performance parameters. The study has revealed the system attains a promising performance of the adsorption refrigeration system using AC / methanol pair driven by solar energy.

Keywords: Adsorption; Refrigeration; Activated carbon/methanol; Simulation

1.0 INTRODUCTION

The utilization of solar energy in the sunlit country is an efficient way to surmount the deficient of energy especially in rural areas where it is sometimes not easy and costly to nourish them with the conservative power grid. Solar refrigeration is the most appropriate application for storing foodstuffs and pharmaceuticals amid solar thermal renovation developments. It is consequently significant to utilize this ordinary reserve predominantly in the field of chilly manufacture. Several scientists and ecologists are in favour of know-how competent in ensuring the environmental prospect of our globe. Alternative systems must employ environmentally sound refrigerants and have the elevated performance to diminish CO_2 emissions contributing to the greenhouse consequence. These ecological harms have given rehabilitated attention to an additional division of sorption refrigeration machines (adsorption and absorption), which signify an attractive substitute in this field. (Benelmirm et al. 2014)

An additional concern with conservative refrigeration skills is the accessibility of power. In rural regions where the conventional electrical energy network is missing, the handling of perishable foodstuffs is a solemn difficulty, particularly in developing nations. The field of application of this form of refrigeration is enormous: the marketable chilly, the freezing agribusiness, the household chilly, and the medical freezing. Some works in the field of adsorption refrigeration and tri-generation have been doing well (Najeh et al. 2016 & 2017) and refrigerators have been recognized (Lingbao et al 2018, Chong et al 2020 & Rouf et al, 2020). Nidal et al.(2010) presented a new design of a solar adsorption refrigeration unit that consists of four adsorbent beds with dissimilar forms of activated carbon (palm seeds, coconut, jojoba seeds, and activated charcoal). Ruud et al. (2010) studied experimentally an adsorption cooling system with the silica gel/water pair. The system consists of two identical adsorbent beds, operating in phase opposition to guarantee the incessant manufacture of chilly. Miyazakia et al

(2009) created a replica of a collection of two-element sorption ice water creation to study the effect of different cycle times on the performance of the collection. Wang and Lu, (2013), analyzed experimentally the impact of heat recuperation and mass on the effectiveness of a chilled water construction unit.

In chilling applications, different types of sorption systems can be employed. Among them, one is the adsorption cycle. Adsorption refrigeration is a thermal-driven refrigeration system, which can be powered by solar energy as well as waste heat (Sumathy et al., 2003). The use of thermal-driven systems facilitates reducing the carbon dioxide discharged from the burning of fossil fuels in power plants. An additional benefit for adsorption systems judged against traditional vapor compression systems is the working fluid utilized. Adsorption systems chiefly employ a natural working fluid such as water and ammonia, which have zero ozone reduction possibility. Najeh et al (2021) presented an experimental investigation of a solar adsorption refrigeration system for three characteristic days. The difference of the solar flux, the typical temperatures of the solar collector as well as the temperatures of the different parts of the adsorption chiller permitted seeing the consequence of the solar flux on the different parameters and the performance of the adsorption chiller.

The sorption refrigeration driven by solar energy fascinated extensive consideration since the heat supply and cool demand is very well matched with the season and the heat quantity. The solid adsorption refrigeration skill driven by solar energy has been examined widely since Tchernev successfully developed the refrigeration system with zeolite–water as the working pair (Tchernev, 1985). Sumathy and Li, (1999) investigated an activated carbon–methanol icemaker powered by solar energy, and results showed that the daily ice production is 4–5 kg and the COP is 0.1–0.2 when the area of the flat plate collector is 0.92m^2. Feng and Tan, (1990; 1991) in South China University of Technology developed the solid adsorption refrigeration system was driven by solar energy, which had a similar performance to the system developed by Sumathy and Li, (1999). Enibe and Iloeje, (1997[a]; 1997[b]) utilized a tubular type of absorber, for which the adsorbent (calcium chloride, activated carbon) is filled inside the metal pipes. The concentric tube arranged at the center of the metal pipe served as the mass transfer channel of the refrigerant, and the metal tube is boned on the collector surface.

Erhard et al., (1998) arranged the condensation part of the horizontal heat pipe inside the adsorbent bed to improve the heat flux density. Headley *et al*. (1994) studied the activated carbon–methanol adsorption refrigerating system utilizing the compound parabolic concentrator (CPC) as the heat source. The system could realize refrigeration even if the solar radiation is very feeble, but the efficiency of the refrigeration system is very low. Wang et al. (2000) developed a compound system of water heaters and refrigerators driven by solar energy to improve energy efficiency. Meanwhile, SJTU developed the silica gel–water adsorption chiller in 2004, which had been applied to the building and grain storage hall with solar energy as the driving power.

2.0 Principle of the Basic Adsorption Refrigeration

The general principle of the fundamental adsorption refrigeration sequence is given in Fig.1. The refrigeration path regularly consists of three major components; a solid adsorbent bed, a condenser, and an evaporator. Several systems utilize isolating valves between the different components and many employ expansion valves between the condenser and the evaporator. The adsorption refrigeration sequence relies largely on the natural affinity of the adsorbent bed (when at low temperature) to draw the refrigerant vapour from the evaporator consequently produces a lower pressure in the evaporator. Once the adsorbent bed is close to the saturation point, the valve between the evaporator and the absorber is closed and heat is applied to the adsorbent bed, therefore liberate the refrigerant vapour which then gets collected and condensed in the condenser before returning to the evaporator. Once this cycle is completed the heat on the adsorbent bed is removed and in some cases, forced cooling is introduced onto the adsorber until the adsorption conditions are established then the valve between the evaporator and the adsorbed is reopened. In the present study, we have designed, fabricated, and tested a single-stage adsorption chiller.

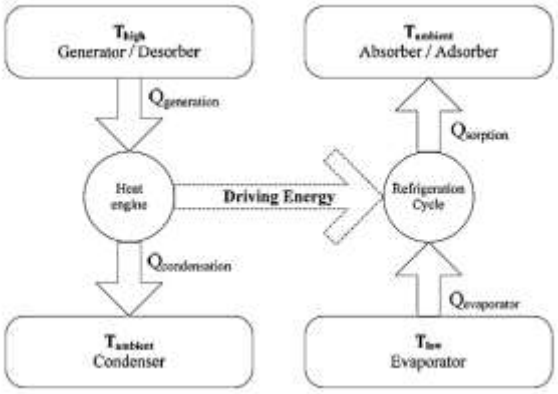

Fig. 1: Principle of the Basic Adsorption Cycle

2.1 System description of adsorption refrigeration system

The adsorption refrigeration system utilizes solid adsorbent beds to adsorb and desorbs a refrigerant to attain the chilling effect. These adsorbent beds filled with solid substance adsorb and desorbs a refrigerant vapour in response to the temperature change of the adsorbent. The fundamental adsorption refrigeration system usually referred to as the adsorption heat drive circle or an adsorption refrigeration path largely consists of four major components: a condenser, a solid adsorbent bed, an evaporator, and an expansion valve.

The adsorbent bed desorbs refrigerant when heated and adsorb refrigerant vapour when cooled. The adsorbent is filled in a hermetically preserved container dyed black for solar emission incorporation at a particular temperature in fulfillment with its condensing pressure. An essential adsorption sequence consists of four thermodynamic steps:

Heating and pressurization A.

The adsorber accepts heat while being closed. The adsorbent temperature enhances, which increases pressure from the evaporation pressure to the condensation pressure. This procedure is corresponding to the "compression" in the compression sequence of line AB in Fig.2.

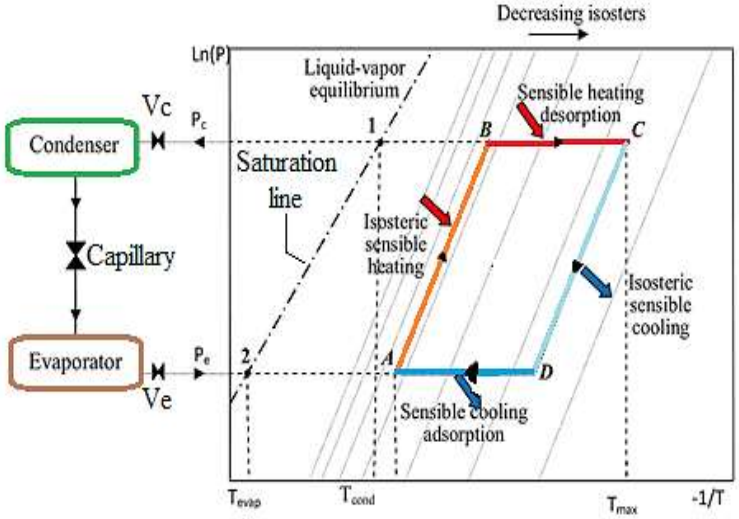

Fig. 2. Clayperon curve of basic adsorption refrigeration cycle.
(Source: Khattab, 2004)

Heating, desorption, and condensation B.

The adsorber continues getting heat while being coupled to the condenser. The adsorbent temperature continues growing, which brings desorption of vapour. This desorbed vapour acquires liquefied in the condenser. This is corresponding to the "condensation" in the compression sequence of line BC in Fig. 2.

Cooling and depressurization C.

During this period, the low-pressure vapour is going into the adsorber from the evaporator. The adsorber liberates heat while being closed. The adsorbent temperature reduces, which diminishes pressure from the condensation pressure down to the evaporation pressure. This procedure is corresponding to the "expansion" in the compression sequence of line CD in Fig. 2.

Cooling, adsorption, and evaporation D.

The adsorber continues to liberate heat while being joined to the evaporator. The adsorbent temperature continues falling, which encourages the adsorption of vapour. This adsorbed vapour is vaporized in the evaporator. The evaporation heat is supplied by the heat cause at a low temperature. This is corresponding to the "evaporation" in the compression sequence of line DA in Fig. 2.

2.2 Mathematical Modeling

The solar-powered adsorption refrigeration system is designed for better effectiveness. A system account is offered after a mathematical representation of the system is developed and a simulation of the design was performed to optimize the design factors.

Performance parameters of adsorption refrigeration system

Fig, 2 is the Clapeyron diagram, and the overall energy achieved by the system during the heating phase Q_T is the addition of the energy Q_{AB} employed to elevate the temperature of the Activated carbon + methanol from point A to B and the energy Q_{BD} utilized for progressive heating of the A.C to point D and desorption of methanol (Khattab, 2004).

$$Q_T = Q_{AB} + Q_{BD} \quad (1)$$

$$Q_{AB} = \left(m_{AC}\, C_{PAC} + C_{Pm} m_{mA}\right)\left(T_B - T_A\right) \quad (2)$$

$$Q_{BD} = \left[\begin{matrix} m_{AC}\, C_{PAC} + \\ C_{pm}\left\{\left(m_{mA} + m_{mD}\right)/2\right\} \end{matrix}\right]\left(T_D - T_B\right) + \left(m_{mA} - m_{mD}\right)H \quad (3)$$

The gross heat released during the cooling phase Q_{e1} is the energy of vaporization of methanol.

$$Q_{e1} = \left(m_{mA} - m_{mD}\right)L \quad (4)$$

But the net energy employed to produce ice Q_e is

$$Q_e = Q_{e1} - Q_{e2} \quad (5)$$

where Q_{e2} is the energy essential for chilling the liquid adsorbate from the temperature at which it is condensed to the temperature at which it fades away.

$$Q_{e2} = \left(m_{mA} - m_{mD}\right)C_{Pm}\left(T_c - T_e\right) \quad (6)$$

Q_{ice1} is the energy necessary to cool water from T_A to 0^oC and to generate ice

$$Q_{ice1} = M^*\left(L^* C_{P\,water}\left(T_A - 0\right)\right), \quad (7)$$

where M* and L* are the mass and latent heat of fusion of ice and net cooling formed is

$$Q_{ice} = M^* L^* \quad (8)$$

Performance estimate

The performance estimate of the closed type adsorption refrigeration system is expressed in terms of (Khattab, 2004)

1. **The collector efficiency** is calculated using eqn (9)
   $$\eta_1 = Q_T / Q_I \quad (9)$$
   where Q_I is the total solar energy contribution to the system during the day.
2. **The evaporator efficiency** is calculated using eqn (10)
   $$\eta_2 = Q_{ice1} / Q_e \quad (10)$$
3. **The cycle coefficient of performance, COP** is calculated using eqn (11)
   $$COP = Q_{e1} / Q_T \quad (11)$$
4. **The net solar coefficient of performance, COP** is calculated using eqn (12)
   $$COP_{net} = Q_{ice} / Q_I \quad (12)$$

Where, Cp is specific heat in kJ/kg K, H is the heat of desorption in kJ/kg, L is the latent heat of evaporation of the methanol in kJ/kg, M is mass in kg, Q is energy in kJ, T is the temperature in ^{o}C.

2.3 Numerical Solution of the Mathematical Models

The mathematical models developed for different parts of the system were utilized to put up a computer algorithm and program in C++ interactive program. Profiles were produced in Microsoft Excel using generated result data from the program, to analyze the influence of evaporation, condensation, and generation temperatures on system effectiveness and to attain optimal values of these temperatures for the adsorbent-refrigerant pair chosen. This simulation permits the COP of the system as a function of the regeneration temperature to be evaluated for different condenser and evaporator temperatures. To estimate the COP for the fundamental refrigeration sequence, the assumptions employed include: the specific heat of dry activated carbon is constant with a value of 711 J/kgK and the specific heat of methanol in the bulk liquid phase is 2534 J/kgK. The specific heat of methanol vapour at constant pressure is 1820 J/kgK, while the specific heat of methanol vapour at constant volume is 1560 J/kgK (Hassan *et al.*, 2011). The physical properties used for Methanol: H = 1400 kJ/kg, L=1100 kJ/kg and Cp_m = 1:34 kJ/kg K., for Charcoal Cp_{AC} = 802:51+ 2:811T J/kg K, where T is in K.

3 RESULTS AND DISCUSSIONS

The results are presented in form of profiles such as pressure developed in the generator, specific cooling power and system coefficient of performance profiles, under varying weather conditions and ambient temperature, operating conditions of evaporating temperature, T_{ev} = 0 ^{o}C, condensing temperature, T_{cond} = 30 ^{o}C and desorption temperature of 100 ^{o}C,

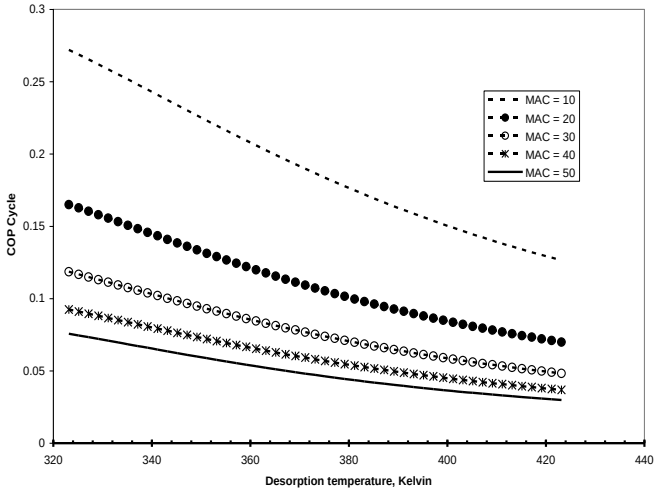

Fig.3. The plot of COP Cycle versus desorption temperature for the different mass of activated carbon

The effect of the amount of mass of activated carbon on the system COP for varying desorption temperatures is shown in Fig.3. It shows that for a given system, there is an optimum generation temperature beyond which the system COP remains constant. This is because heating beyond the optimum generation temperature does not result in commensurate desorption of refrigerant, rather it increases the sensible heat gained by the adsorbent bed. These results in a longer cooling time required at the end of desorption.

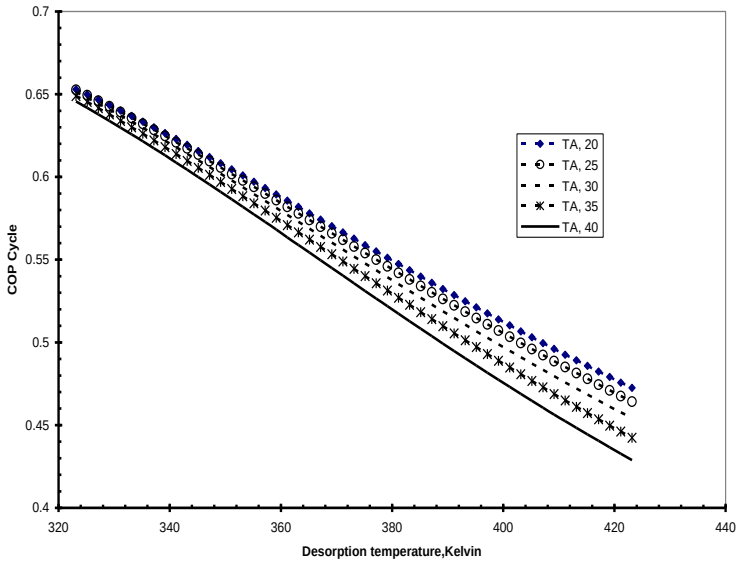

Fig.4. The plot of COP Cycle versus desorption temperature for different ambient temperature

The effect of ambient temperature on the system COP for varying desorption temperatures is shown in Fig.4. It shows that for a given system, as the ambient temperature reduces, for a given condenser temperature, 30 ^{o}C the COP reduces, and as the desorption temperature reduces, however the COP increases, that is a higher regeneration temperature is required for the same value of COP. This is because the energy required raising the temperature from evaporation temperature, T_{ev} to condensation temperature, T_{cond} increases as reflected in the higher desorption temperatures.

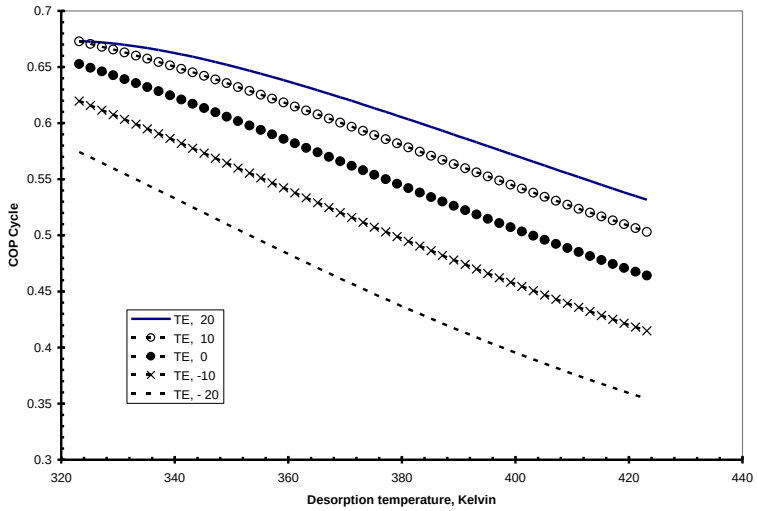

Fig.5. The plot of COP Cycle versus desorption temperature for different evaporator temperature

From the simulation results presented in Fig.5, for the activated carbon-methanol pair, as the evaporator temperature reduces, for a given condenser temperature, 30 ^{o}C the COP reduces for a given regeneration temperature, 120 ^{o}C, that is a higher regeneration temperature is required for the same value of COP. This is because the energy required raising the temperature from evaporation temperature, T_{ev} to condensation temperature, T_{cond} increases as reflected in the higher desorption temperatures.

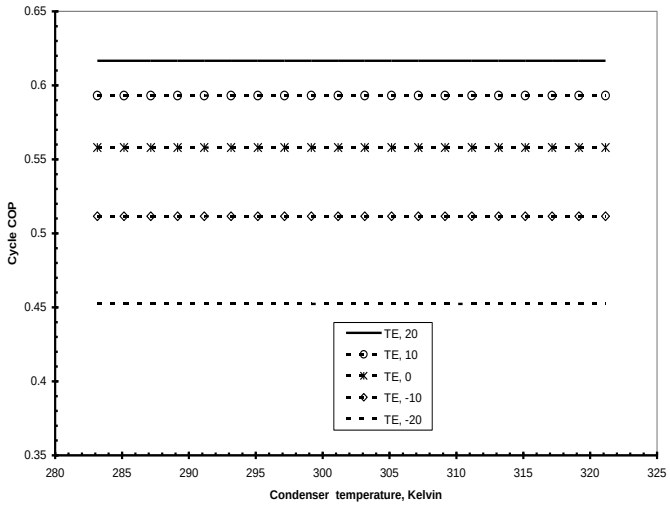

Fig.6. The plot of cycle COP versus condenser temperature for different evaporator temperature

Fig.6. Shows effect of evaporation temperature on the system COP for varying condensation temperatures. It shows that as evaporation temperature increases, the COP increases but there is no appreciable change with varying condenser temperature. It is shown clearly that for different evaporation temperatures there is an appreciable corresponding effect on COP of the system.

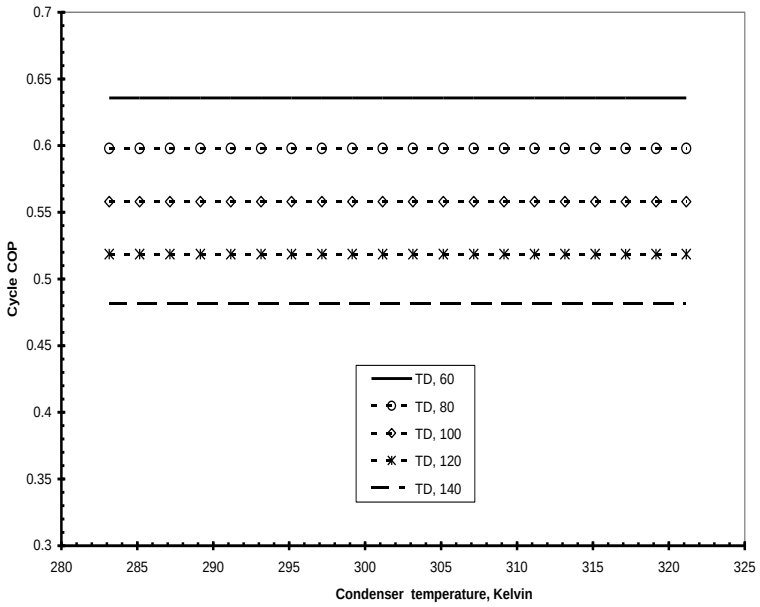

Fig.7. The plot of cycle COP versus condenser temperature for different desorption temperature

Fig.7. shows the effect of condenser temperature and desorption temperature on the cycle coefficient of performance. As desorption temperature increases, the COP reduces but there are no appreciable changes with varying condenser temperatures. It is shown clearly that for different desorption temperatures there is an appreciable effect on COP of the system. Condenser temperature has no appreciable effect on the cycle coefficient of performance. This is because heating beyond the optimum generation temperature does not result in commensurate desorption of refrigerant, rather it increases the sensible heat gained by the adsorbent bed. This result in a longer cooling time required at the end of desorption.

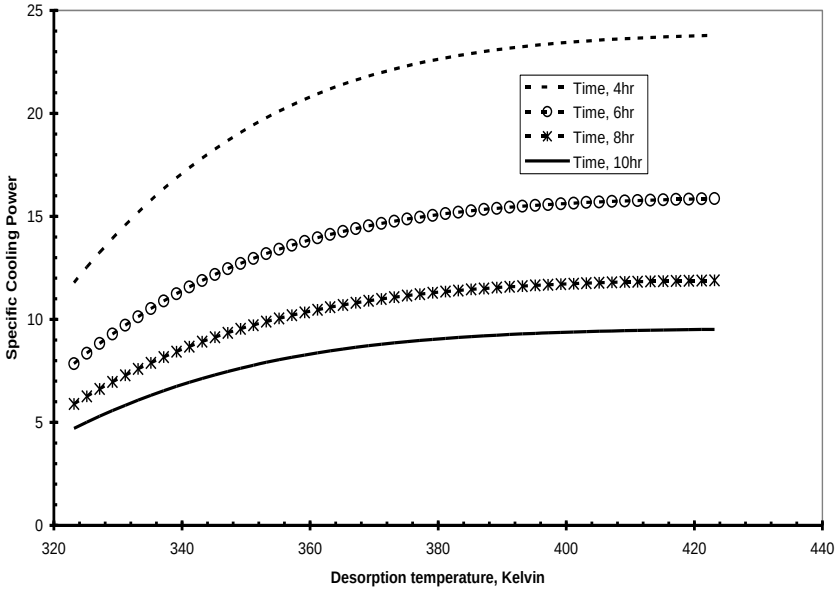

Fig.8. The plot of specific cooling power versus desorption temperature

Fig.8. shows the effect of cooling duration and desorption temperature on the specific cooling power, SCP. The figure shows that the SCP has appreciable changes with varying cooling durations, 4hrs, 6hrs, 8hrs, and 10hrs and for a very small desorption temperature, the specific cooling power is small. As cooling duration increases, the SCP reduces but there is no appreciable increase in specific cooling power beyond a desorption temperature of 380 K, It indicates that the system performs better at a small cooling duration which occurs when there is a harsh weather condition, high solar intensity

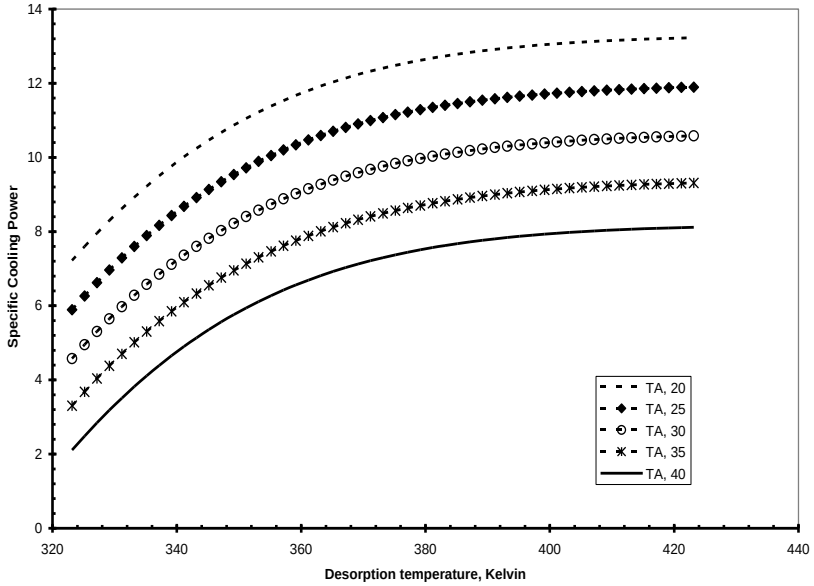

Fig.9. The plot of SCP versus desorption temperature for different ambient temperature

Fig.9. shows the effect of ambient temperature and desorption temperature on the specific cooling power, SCP. The figure shows that the SCP has appreciable changes with varying ambient temperature, 20 ^{o}C, 25 ^{o}C, 30 ^{o}C, 35 ^{o}C, and 40 ^{o}C and for a very small desorption temperature, the specific cooling power is small. As ambient temperature increases, the SCP reduces but there is no appreciable increase in specific cooling power beyond a desorption temperature of 380 K, It indicates that the system performs better at small ambient temperature which occurs when there is a harsh weather condition, high solar intensity

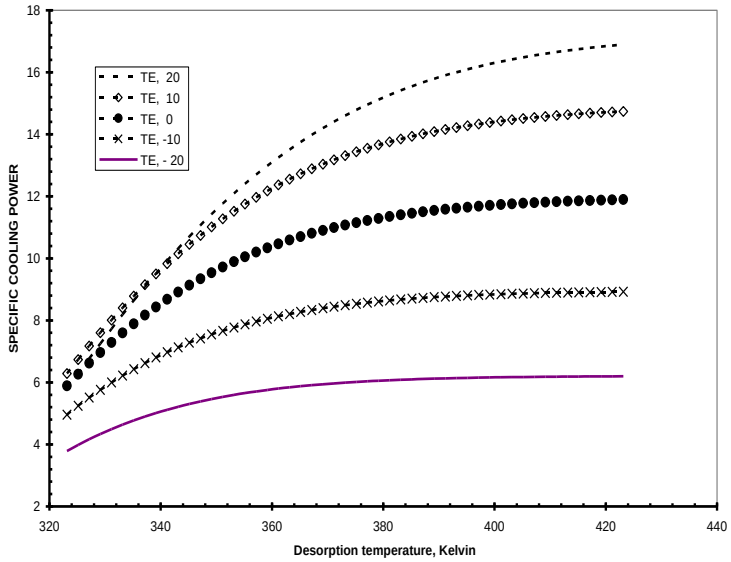

Fig.10. The plot of specific cooling power versus desorption temperature for different evaporator temperature

From the simulation results presented in Fig.10, for the activated carbon-methanol pair, as the evaporator temperature reduces, for a given condenser temperature, the specific cooling power, SCP reduces for a given regeneration temperature i.e. a higher regeneration temperature is required for the same value of SCP. This is because the energy required to raise the temperature from T_{ev} to T_{cond} increases as reflected in the higher desorption temperatures.

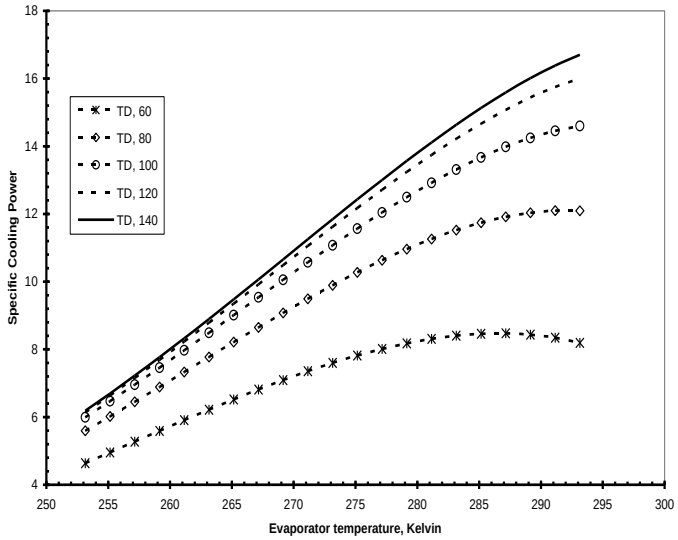

Fig.11. The plot of specific cooling power versus evaporator temperature for different desorption temperature

Fig.11. shows the change in specific cooling power, SCP as a function of evaporator temperature for different desorption temperatures (60 ^{o}C, 80 ^{o}C, 100 ^{o}C, 120 ^{o}C, and 140 ^{o}C,) respectively. The figure shows that for very small evaporator temperatures, the specific cooling power is small for different desorption temperatures. As the evaporator temperature increases, the SCP increases with an increase in desorption temperature. For the chosen evaporator temperature of 273 K however, there is no appreciable increase in specific cooling power beyond a desorption temperature of 120 ^{o}C. The evaporator temperature however increases with an increase in desorption temperature.

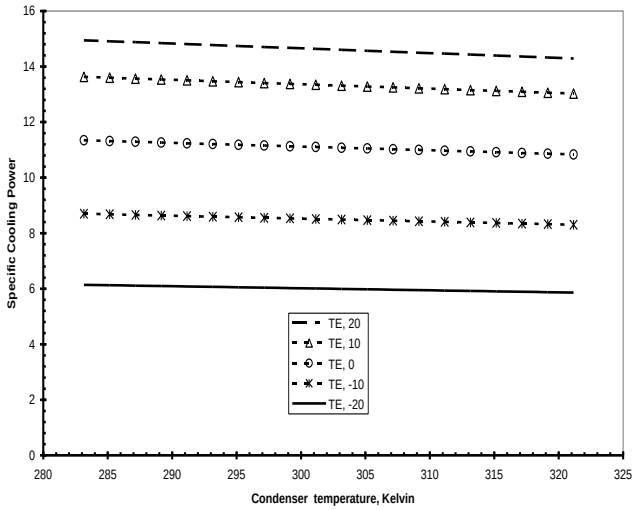

Fig.12. The plot of specific cooling power versus condenser temperature for different evaporator temperature

Fig.12. shows the change in specific cooling power, SCP as a function of condenser temperature for different evaporator temperatures (20 ^{o}C, 10 ^{o}C, 0 ^{o}C, -10 ^{o}C, and -20 ^{o}C,) respectively. The figure shows that for very small evaporator temperatures, the specific cooling power is small. As the evaporator temperature increases, the SCP increases with no appreciable effect of different condenser temperatures. Condenser temperature has no appreciable effect on specific cooling power.

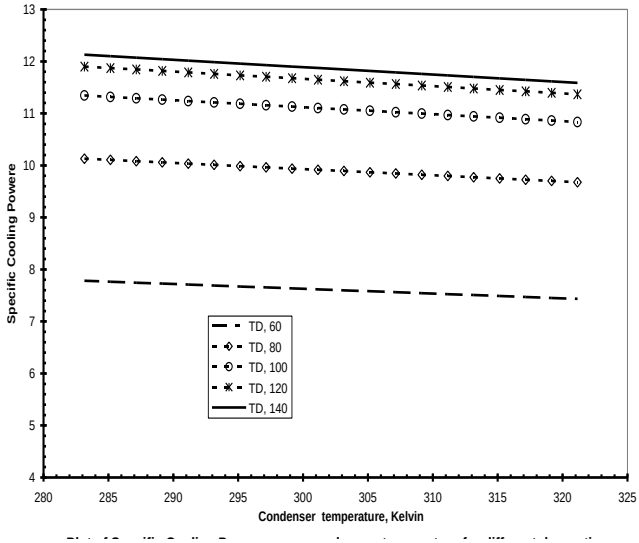

Fig.13. The plot of specific cooling power versus condenser temperature for different desorption temperature

Fig.13. shows the effect of desorption temperature and condenser temperature on the specific cooling power, SCP. The figure shows that for a very small desorption temperature, the specific cooling power is small. As desorption temperature increases, the SCP increases but there is no appreciable increase in specific cooling power beyond a desorption temperature of 120 ^{o}C, It signifies desorption operating temperature for methanol to cease function as adsorbate in activated carbon methanol pairs but acting as a catalyst. The SCP shows no appreciable changes with varying condenser temperatures. It is shown clearly that for different desorption temperatures below 120 ^{o}C there is an appreciable effect on the specific cooling power of the system.

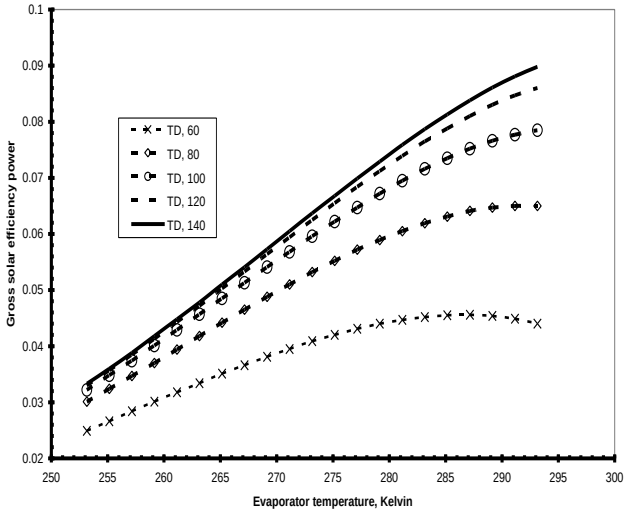

Fig.14. The plot of gross solar efficiency power versus evaporator temperature for different desorption temperature

Fig.14. shows the effect of desorption temperature and evaporation temperature on gross solar efficiency power. The figure shows that for very small desorption and evaporation temperatures, the gross solar efficiency power is small. As desorption and evaporation temperature increase, the gross solar efficiency power increases but there is no appreciable increase in gross solar efficiency power beyond a desorption temperature of 120 ^{o}C, It signifies desorption operating temperature for methanol to cease function as adsorbate in activated carbon methanol pairs but acting as a catalyst. It is shown clearly that for different desorption temperatures below 120 ^{o}C there is an appreciable effect on the system performance.

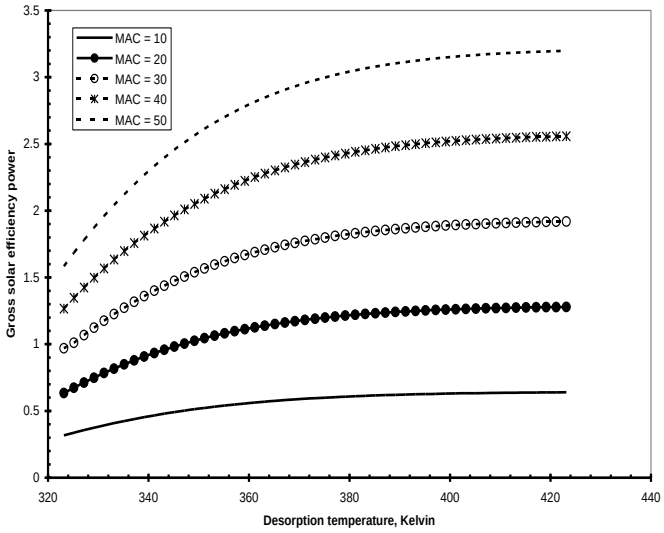

Fig.15. The plot of gross solar efficiency power versus desorption temperature for the different mass of activated carbon

The effect of the amount of mass of activated carbon in the generator on the gross solar efficiency power for varying desorption temperatures is shown in Fig.15. It shows that for a given system, there is an optimum generation temperature beyond which the gross solar efficiency power remains constant. This is because heating beyond the optimum generation temperature does not result in commensurate desorption of refrigerant, rather it increases the sensible heat gained by the adsorbent bed. This result in a longer cooling time required at the end of desorption. It is shown clearly that for a different amount of mass of activated carbon in the generator, there is a significant corresponding effect on gross solar efficiency power

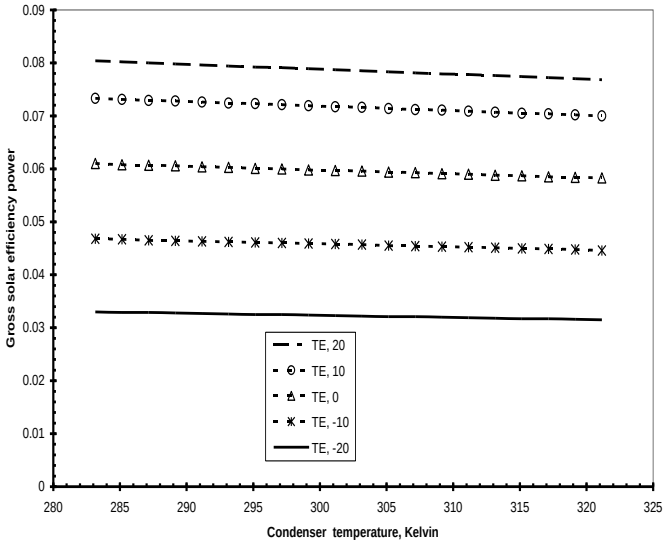

Fig.16. The plot of gross solar efficiency power versus condenser temperature for different evaporator temperature

Fig.16 shows the effect of evaporation temperature and condensation temperature on the gross solar efficiency power. The figure shows that for very small evaporation temperatures, gross solar efficiency power is small. As the evaporation temperature reduces, the gross solar efficiency power reduces. The gross solar efficiency power shows no appreciable changes with varying condensation temperatures. It is shown clearly that different evaporation temperatures have a significant effect on the gross solar efficiency power of the system.

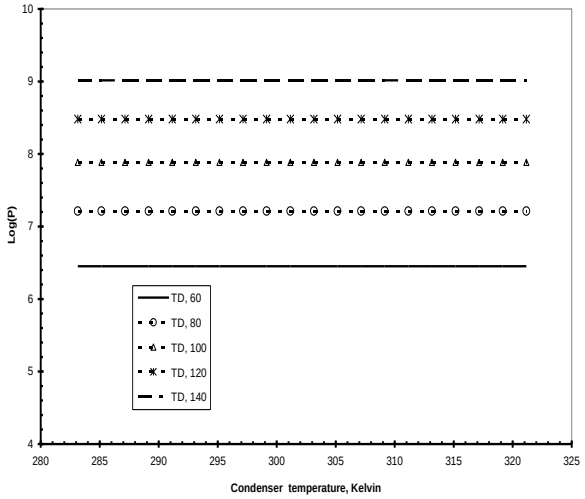

Fig.17. The plot of log(P) versus condenser temperature for different desorption temperature

Fig.17. shows the effect of condenser temperature and desorption temperature on the adsorber pressure. The figure shows that for a very small desorption temperature, the adsorber pressure is small. As desorption temperature increases, the pressure increases. The system pressure shows no appreciable changes with varying condenser temperatures. It is shown clearly that different desorption temperatures have a significant effect on pressure developed in the generator.

4. CONCLUSIONS

The system performance is appraised in terms of system performance parameters such as specific cooling power (SCP), refrigeration cycle COP (COP_{cycle}), and solar coefficient of performance (COPs), which were evaluated by a simulation computer program. The effects of climatic governing parameters on system performance parameters are being investigated.

The influences of some important operating and design parameters on the system performance are significant. The results revealed that there is desorption optimum operating temperature for methanol to cease

function as adsorbate in activated carbon methanol pairs but acting as a catalyst. The system performance shows no appreciable changes with varying condenser temperature with significant effect with varying evaporation and desorption temperature. It is shown clearly that for different desorption temperatures below 120 ^{o}C there is an appreciable effect on the system performance parameters. This work has revealed that the system can attain a promising performance on the adsorption refrigeration systems driven by solar energy.

Reference

Benelmir R., Ghilen N., El Ganaoui M., Descieux D., and Gabsi S., (2014) Technology Platform ENERBAT - Gas Cogeneration, Solar Heating, and Cooling, Int. J. of Thermal & Environmental Engineering Vol. 7, No. 2 pp.79-85

Dieng A.O. & Wang R.Z. (2001) Literature review on solar adsorption technologies for ice-making and air conditioning purposes and recent developments in solar technology. Renew Sustain Energy Rev; 5(4):313–42,

Enibe, S.O., and Iloeje, O.C. (1997[a]) Design optimization of the flat plate collector for a solid absorption solar refrigerator. Solar Energy, 60(2), 77–87.

Enibe, S.O., and Iloeje, O.C. (1997[b]) Transient analysis and performance prediction of a solid absorption solar refrigerator. Solar Energy, 60(1), 43–59.

Erhard, D., Spindler, K. and Hahne, E. (1998) Test and simulation of a solar-powered solid sorption cooling machine. International Journal of Refrigeration, 21(2), 133–141.

Feng, Y. and Tan, Y.K. (1990). The research for the adsorption refrigeration cycle with activated carbon-methanol as the working pair. Journal of Refrigeration, (1), 1–5, ISSN: 0253–4339

Feng, Y. and Tan, Y.K. (1991) Research on the heat and mass transfer performance for the adsorption refrigeration systems. Journal of Chemical Industry and Engineering, 42(3), 342–347, ISSN: 0438-1157

Najeh G., Gabsi S, Ganaoui M. E, Benelmir R. (2021) Experimental Analysis of a Solar Adsorption System Refrigeration Cycle with Silica-Gel/Water Pair, Journal of Fundamentals of Renewable Energy and Applications, Vol.11 No.1 pp1-7

Habib K, Saha B.B., Chakraborty A, Oh S.T., & Koyama S. (2013) Study on solar-driven combined adsorption refrigeration cycles in a tropical climate. Applied Thermal Engineering; 50(2): 1582–1589

Headley, S., Kothdiwal, A.F., McDoom, I.A. (1994) Charcoal-methanol adsorption refrigerator powered by a compound parabolic concentrating solar collector. Solar Energy, 53(2), 191–197.

Khattab, N.M. (2004) A novel solar-powered adsorption refrigeration module Applied Thermal Engineering 24 (2004) 2747–2760

Miyazakia T., Akisawa A., Saha B.B., El-Sharkawy I.I., & Chakraborty A., (2009), "A new cycle time allocation for enhancing the performance of two-bed adsorption chillers", International Journal of Refrigeration, Vol. 32, (pp. 846 – 853.

Najeh G., Messai S, Gabsi S, Ganaoui M. E. & Benelmir R, (2017), Performance Simulation of Two-Bed Silica Gel-Water Adsorption Chillers, Global Journal of Researches in Engineering: J General Engineering Vol. 17 Issue 3 Version 1.0 pp.41-49.

Nidal H. Abu H., & Mu'taz A. A., (2010). Optimization of solar adsorption refrigeration system using experimental and statistical techniques, Energy Conversion and Management 51, pp.1610–1615.

Rouf R.A., Jahan N., KAlam.C.A., Sultan A.A., Saha B.B., & Saha S.C., (2020). "Improved cooling capacity of a solar heat-driven adsorption chiller", Case Studies in Thermal Engineering, Vol. 17,

Ruud J.H., Grisel, S. F. Smeding, R. B.; (2010), Waste heat driven silica gel/water adsorption cooling in trigeneration; Applied Thermal Engineering 30, pp.1039–1046.

Sumathy K, Yeung K.H, & Yong L. (2003) Technology development in the solar adsorption refrigeration systems. Prog Energy Combust Sci; 29 (4): 301–27,

Sumathy, K. and Li, Z.F. (1999) Experiments with solar-powered adsorption ice maker. Renewable Energy, 16, 704–707.

Tchernev, D. (1985) Heat pump energized by low-grade heat sources. US Patent PCT/US85/00783.

Wang R.Z., and Lu Z.S., (2013), "Performance improvement by mass-heat recovery of an innovative adsorption air-conditioner driven by 50-80°C hot water", Applied Thermal Engineering, Vol. 55, pp.113-120

Wang L., Bu X., & Ma W., (2018), "Experimental study of an Adsorption Refrigeration Test Unit " Energy Procedia, vol. 152, pp. 895-903

Wang, R.Z., Li, M., Xu, Y.X. & Wu, J.Y. (2000). An energy-efficient hybrid system of solar-powered water heater and adsorption ice maker. Solar Energy, 68(2), 189–195.

Zhao C., Wang Y, Li M, Zhao W, Li X, Du W, &Yu Q, (2020) Experimental study of a solar adsorption refrigeration system integrated with a compound parabolic concentrator based on an enhanced mass transfer cycle in Kunming, China, Solar Energy, vol. 195pp.37–46.